# The neutral drag coefficient over polar sea ice with small floes and/or melt ponds


Christof Lüpkes, Vladimir M. Gryanik, Jörg Hartmann

*Alfred Wegener Institute for Polar and Marine Research, Bremerhaven, Germany*



## Abstract

Neutral drag coefficients observed over polar sea ice show a large variability, since the aerodynamical roughness of sea ice depends on quantities like sea ice concentration *A*, ice freeboard ($h_f$, $h_p$), characteristic length of floes and melt ponds ($D_i$, $D_w$) which are all variable in space and time. Attempts have been made in the past to relate the surface drag solely on sea ice concentration, since the latter can be determined most easily in coupled atmosphere sea ice models.

Such a surface drag parametrization is derived here for the marginal sea ice zones with floe lengths smaller than 1 km and in analogy to an idea of Andreas et al. (2010) also for the summertime inner Arctic sea ice covered with melt ponds. This is done on a physical basis with the demand to use only few assumptions on the floe and melt pond geometry and the distribution of both. Our model is based on the splitting of total surface drag into contributions of skin drag over open water and ice and of form drag, so that

$$C_{dn10} = (1-A)\,C_{d,w} + A\,C_{d,i} + C_{d,f}$$

, where $C_{d,w}$ and $C_{d,i}$ are the skin drag coefficients over open water and sea ice, respectively and $C_{df}$ describes form drag. It is caused by the dynamical pressure occurring due to the different elevations of sea ice and open water surfaces. In the marginal sea ice zones the surface elevations are dominated by the freeboard of the drifting floes, while during summer the different surface levels of sea ice and open water in the melt ponds/leads are generating form drag. It is shown here that the form drag coefficients can be derived as

$$C_{d,f} = \frac{c_w}{2}\left[\frac{\ln(h_f/z_{0,w})}{\ln(10/z_{0,w})}\right]^2 S_c^2\,\frac{h_f}{D_i}\,A$$

for the MIZ and as

$$C_{d,f} = \frac{c_w}{2}\left[\frac{\ln(h_p/z_{0,w})}{\ln(10/z_{0,w})}\right]^2 S_c^2\,\frac{h_p}{D_w}\,(1-A)$$

for summer sea ice with melt ponds,

$z_{0,w}$ is the surface roughness of open water, $S_c$ is a sheltering function, $c_w$ is the coefficient of resistance of a single ice obstacle. Applying simplifications which are partly based on airborne and satellite observations of sea ice morphology the following approximations of these equations are obtained which can be easily applied in weather prediction and climate models

For the MIZ we obtain $C_{d,f} = C_f\,(A_* - A)^\beta A$

and for summer sea ice with melt ponds $C_{d,f} = C_f\,\dfrac{h_1\,(1-A)^2}{a_1 + a_2\,(1-A)}$ with the constants $C_f$, $h_1$, $a_1$, $a_2$, $\beta$.


## Conclusions

A new parametrization of the neutral drag coefficients over the marginal sea ice zone and summer sea ice with melt ponds was derived on the basis of the skin drag / form drag concept. The principal method is similar to a previous work by Lüpkes and Birnbaum (2005), but the present physically based derivation of form drag needs less assumptions on the floe characteristics and results in a formulation which is simple enough to be applied efficiently to climate models. Governing parameters besides the sea ice concentration *A* are the characteristic edge lengths $D_i$ of floes and $D_w$ of melt ponds as well as freeboard, where the sensitivity on the latter is smaller than the sensitivity on the other parameters.

The most important result is that although the sea ice pattern with floes in the MIZ and melt ponds in summer sea ice looks at a first glance very similar, the different morphology results in general in different formulae for the drag coefficients with different functional dependences on the sea ice concentration. However, special conditions and special distributions of floe sizes and melt pond sizes, respectively, exist, where the dependence on the sea ice concentration is identic for the MIZ and summer sea ice with melt ponds.

A simple quadratic polynomial fit given by Andreas et al. (2010) can be obtained only for special cases of floe and melt pond distributions and using constant surface roughness lengths over open water and sea ice.


### References

Anderson, R.J., 1987: Wind Stress Measurements over Rough Sea Ice During the 1984 Marginal Ice Zone Experiment', J. Geophys. Res. 92(C7), 6933-6941.

Andreas, E.L., Horst, T.W., Grachev, A.A., Persson, P.O.G., Fairall, C., Guest, P., and R.E. Jordan, 2010: Parametrizing turbulent exchange over summer sea ice and the marginal ice zone, Q.J.R. Meteorol. Soc., 136, 927-943

Andreas, E.L., Tucker, W.B. and Ackley, S.F., 1984: Atmospheric Boundary-Layer Modification, Drag Coefficient, and Surface Heat Flux in the Antarctic Marginal Ice Zone, {J. Geophys. Res., 89 (NC1)}, 649-661.

Fetterer , F., S. Wilds, and J. Sloan, 2008: Arctic sea ice melt pond statistics and maps, 1999-2001. Boulder, Colorado USA: National Snow and Ice Data Center. Digital media.

Hartmann, J., Kottmeier, C., Wamser, C., Augstein, E., 1994: Aircraft Measured momentum, heat and radiation fluxes over Arctic se ice, in: The polar ocean and their role in shaping the global environment, Geophys. Monogr., 85, 443-454

Kottmeier, C., Hartmann, J. et al., 1994: Radiation and eddy flux experiment 1993 (REFLEX II), Reports on Polar Research, Alfred Wegener Institute, Bremerhaven, 133, 62 pp.

Lüpkes, C., and G. Birnbaum, G., 2005: Surface drag in the Arctic marginal sea ice zone: a comparison of different parameterisation concepts, Boundary-Layer Meteorol., 117(2), 179-211



### Acknowledgements:

We thank NSIDC for the data on melt ponds (Fetterer et al., 2008). Part of this work was funded by DFG (Grant No. LU 818/3-1)



Corresponding author: Christof.Luepkes@awi.de


## Derivation of equations for form drag as a function of sea ice concentration

The morphological structures of the sea ice/open water surface in the marginal sea ice zones and over summer sea ice with melt ponds and/or leads differ from each other and thus different equations result for the form drag (dynamical pressure on floe edges and edges of sea ice at melt ponds.).

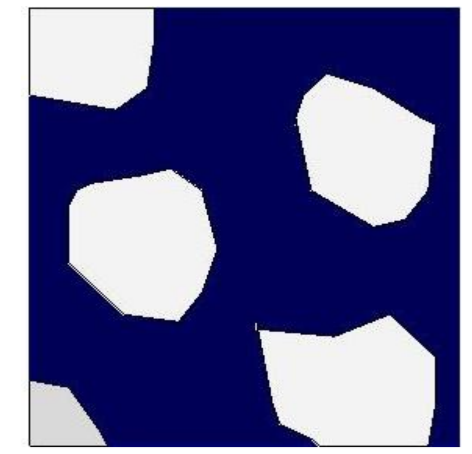

Surface morphology over the marginal sea ice zone. Floes can be clearly identified.

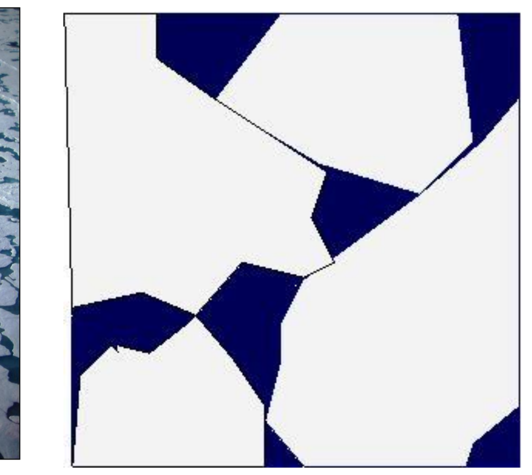

Summer sea ice conditions with melt ponds. Especially in the initial state of melting ponds can be more clearly identified than floes.

### Marginal sea ice zone

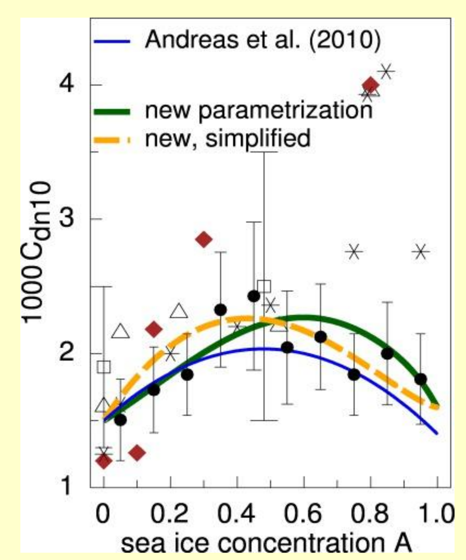


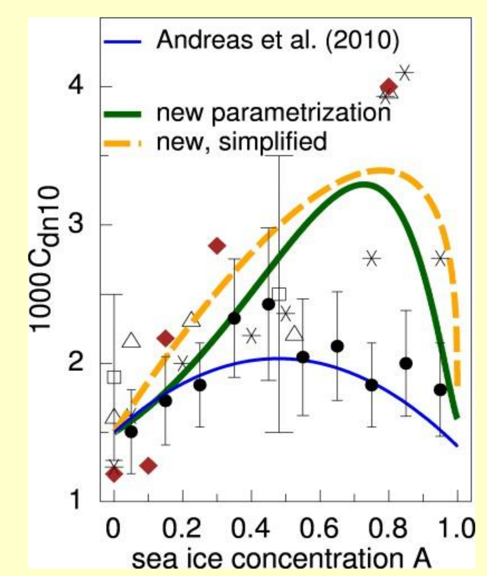


Results of the new parametrization in both figures differ by the used value of $\beta$ (1.4 (left) and 0.3 (right)).

Symbols represent observations of Hartmann et al. (1994), Kottmeier et al. (1994) (black dots); Anderson (1987) (asterisks); Andreas et al. (1984) (red diamonds); Guest and Davidson (1987) (triangles).

**Assumptions:**

N quadratic floes with edge length $D_i$ and freeboard $h_f$ in area $S_t$. The sea ice concentration A is then given by $A = N D_i^2 / S_t$ and form drag is given by

$$F_d = \frac{\rho}{2} c_w \underbrace{\frac{1}{N}\frac{S_c^2}{h_f D_i}\sum\left[\int_0^{D_i}\int_{z_0}^{h_f} u^2\,dz\,dy\right]}_{P'} \frac{N h_f D_i}{S_t} = \frac{\rho}{2} c_w P' \frac{h_f}{D_i} A$$

$S_c$ = Sheltering function, U = wind speed, $c_w$ = coefficient of resistance of individual floes, $z_{0,w}$ = surface roughness length over open water

Assuming a logarithmic wind profile and some straightforward approximations, after integration:

$$C_{dn10} = (1-A)C_{d,w} + AC_{d,i} + \frac{c_w}{2}\left[\frac{\ln(h_f/z_{0,w})}{\ln(10/z_{0,w})}\right]^2 S_c^2\,\frac{h_f}{D_i}A$$

This parametrization depending on the floe aspect ratio $h_f/D_i$ can be used in such climate models which predict ice thickness and floe length. Using alternatively a linear fit of observed freeboard (AWI campaign REFLEX over the MIZ) and the fit

$$D_i = \frac{D_0}{(A_* - A)^\beta}$$

($D_0$ = constant)

to observed floe lengths, we obtain

$$C_{dn10} = (1-A)\,C_{d,w} + A\,C_{d,i} + C_f\,(A_* - A)^\beta A \qquad C_f = \frac{c_w}{2}\left[\frac{\ln(h_{fl}/z_{0,w})}{\ln(10/z_{0,w})}\right]^2 S_c^2\,\frac{h_{fl}}{D_0}$$

$A_*$ is close to 1 and depends on minimum and maximum floe lengths in the MIZ.

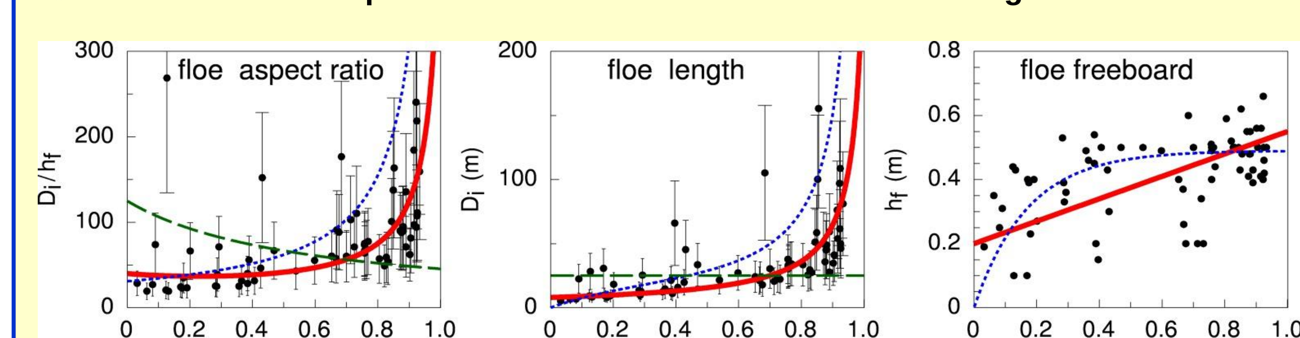


Symbols show observations of Hartmann et al. (1994) and Kottmeier et al. (1993). Red line in the floe length figure represents the above fit of $D_i$ and a linear fit of freeboard. A constant floe lenght (green line) does not result in the observed floe aspect ratio $D_i/h_f$.

### Inner Arctic with melt ponds

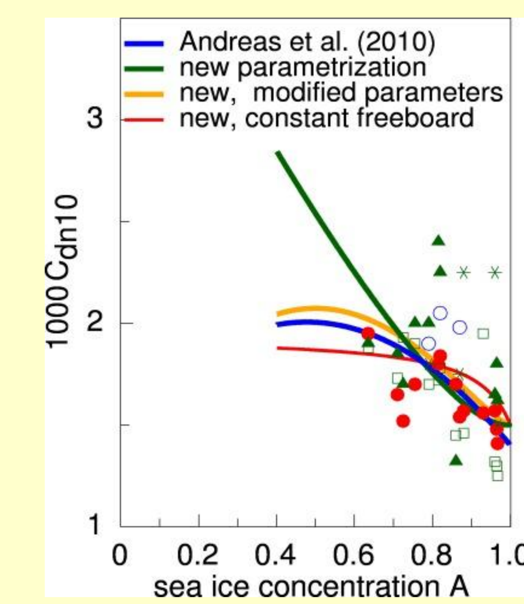


Observations (symbols) are from SHEBA. They have been (roughly) copied here from Figure 3 of Andreas et al (2010). (red dots refer to the results at the ASFG tower, which are according to Andreas et al. (2010) the most reliable data).

The Andreas et al. (2010) parametrization for the inner Arctic and MIZ represents a polynomial fit to the MIZ observations (left yellowcolumn) and to the observations shown in this figure.

**Assumptions:**

$N_p$ quadratic melt ponds with edge length $D_w$, and ice freeboard (relative to pond surface) hf in area $S_t$

Open water concentration 1-A is then given by $1-A = D_w^2 N_p / S_t$ and we obtain

$$C_{dn10} = (1-A)C_{d,w} + AC_{d,i} + \frac{c_w}{2}\left[\frac{\ln(h_p/z_{0,w})}{\ln(10/z_{0,w})}\right]^2 S_c^2\,\frac{h_p}{D_w}(1-A)$$

Assuming that freeboard $h_p$ depends linearly on (1-A) with $h_p = h_1$ (1-A) and based on satellite observations of melt ponds (Fetterer et al. , 2008) (see Figure below) we obtain

$$D_w = a_1 + a_2\,(1-A)$$

This results in:

$$C_{dn10} = (1-A)\,C_{d,w} + A\,C_{d,i} + C_f\,\frac{h_1\,(1-A)^2}{a_1 + a_2(1-A)} \qquad C_f = \frac{c_w}{2}\left[\frac{\ln(h_1 A(1-A)/z_{0,w})}{\ln(10/z_{0,w})}\right]^2 S_c^2$$

($h_1$, $a_1$, $a_2$ are constants).

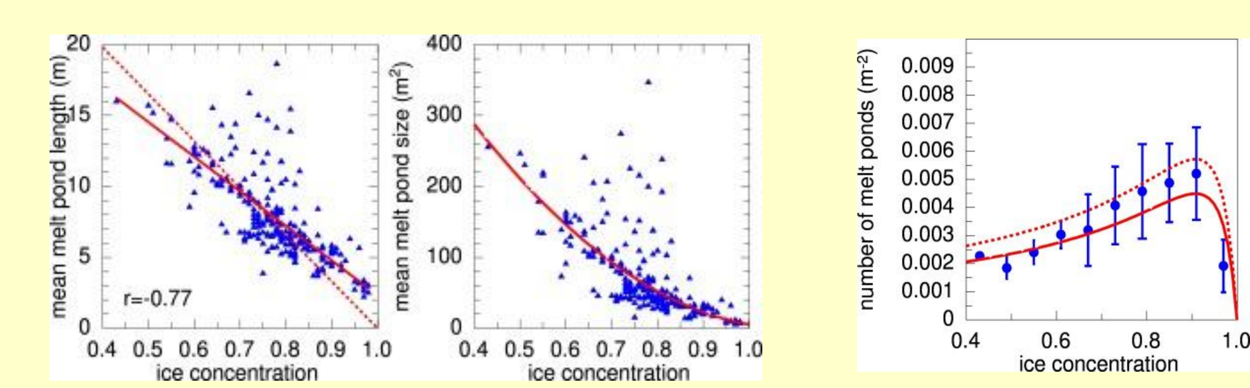


Symbols represent data analysed on the basis of satellite observations (Fetterer et al., 2008). Parametrized number densities (red) result with different assumptions on floe geometry on the basis of parametrized $D_w$ .